

STATE OF THE CLIMATE IN 2016

A photograph of a woman in a pink shirt and dark skirt planting seedlings in a field of red soil. The field is filled with rows of small green plants. In the background, there are trees and a cloudy sky.

Special Supplement to the
Bulletin of the American Meteorological Society
Vol. 98, No. 8, August 2017

ing trend as El Niño waxes and slower than that trend when El Niño wanes (Johnson and Birnbaum 2017). The rapid increase in OHCA in 2015 followed by a reduction in 2016 is thus consistent with the transition from a strong El Niño in early 2016 to borderline La Niña conditions in late 2016. Net OHCA appears to plateau in 2016 from 700 to 2000 m (Fig. 3.6b). Causes of the differences among estimates are discussed in Johnson et al. (2015a). From 2000 to 6000 m (Fig. 3.6b), trends are estimated from differences between decadal surveys (Desbruyères et al. 2016).

The rate of heat gain from linear trends fit to each of the five global integral estimates of 0–700 m OHCA from 1993 through 2016 (Fig. 3.6a) range from 0.34 (± 0.06) to 0.42 (± 0.17) W m^{-2} applied over the surface area of Earth (Table 3.2). Linear trends from 700 to 2000 m over the same time period range from 0.24

(± 0.08) to 0.31 (± 0.03) W m^{-2} . All trends in the upper two layers agree within uncertainties. For 2000–6000 m, the linear trend is 0.07 (± 0.04) W m^{-2} from 1992 to 2009. Summing the three layers (with their slightly different time periods), full-depth ocean heat gain rate ranges from 0.65 to 0.80 W m^{-2} .

d. *Salinity*—G. C. Johnson, J. Reagan, J. M. Lyman, T. Boyer, C. Schmid, and R. Locarnini

1) INTRODUCTION—G. C. Johnson and J. Reagan

Salinity patterns, both means and their variations, reflect ocean storage and transport of freshwater, a key aspect of global climate (e.g., Rhein et al. 2013). Long-term means of sea surface salinity (SSS) are largely determined by patterns of evaporation, precipitation, and river runoff (e.g., Schanze et al. 2010), modified by advection and entrainment (e.g., Yu

SIDEBAR 3.1: CHANGES IN THE NORTHEAST U.S. SHELF ECOSYSTEM AND FISHERIES—J. HARE

The pace of observed change in the northeast U.S. shelf ecosystem, which extends from Cape Hatteras, North Carolina, through the Gulf of Maine, is faster than in many other continental shelf ecosystems (Pershing et al. 2015). Future change in the northeast U.S. shelf ecosystem also is projected to be greater than in many other portions of the world's oceans (Saba et al. 2016). Temperatures have risen $\sim 1.5^\circ\text{C}$ in this region since 1995 (Fig. SB3.1). Some of this temperature rise is attributable to long-term climate change and some of it is attributable to natural variability related to the Atlantic multidecadal oscillation. The region is also a “hotspot” for sea level rise: increases in the rates of sea level rise are ~ 3 –4 times higher in this region compared to the global average (Sallenger et al. 2012). There are also changes in the Gulf Stream, with increased variability in the Gulf Stream path north of Cape Hatteras (Andres 2016) and recently observed direct interactions with the northeast U.S. shelf (Gawarkiewicz et al. 2012).

The northeast U.S. shelf ecosystem supports a wide array of living marine resources, from Atlantic sea scallops, one of the most valuable, to the North Atlantic right whale, one of the most endangered. All of these resources—fish, invertebrates, marine mammals, sea turtles, plants, habitats, and other ecosystem components—are being impacted by changing ocean and climate conditions in the region. The productivity of some species has been linked to temperature, with some species exhibiting decreased productivity related to warming (e.g., Atlantic cod, Fogarty et al. 2008; winter flounder, R. Bell et al. 2014) and other species exhibiting increased productivity (e.g., Atlantic croaker, Hare et al. 2010). Still other species have shown no change in productivity during the recent period of

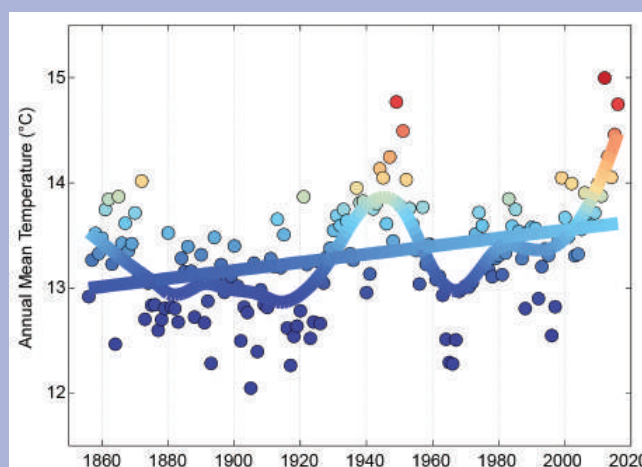


FIG. SB3.1. Mean annual temperature ($^\circ\text{C}$, colors) on the northeast U.S. shelf ecosystem (36 – 46°N , 76 – 66°W) derived from the ERSSTv4 dataset (www.esrl.noaa.gov/psd/data/gridded/data.noaa.ersst.v4.html). Long-term change is estimated with a linear regression (straight line) and multidecadal variability is estimated with a loess smoother. As depicted, the temperatures, as indicated on the y-axis, transition from dark blue (lowest) to red (highest).

warming (e.g., summer flounder, R. Bell et al. 2014). This range of responses suggests that some species in the region will be negatively impacted by changes in ocean and climate conditions and other species will be positively impacted.

Changes in marine species distributions have been widely documented in the northeast U.S. shelf ecosystem. Long-term bottom trawl surveys provide an important data source for

CONT. SIDEBAR 3.1: CHANGES IN THE NORTHEAST U.S. SHELF ECOSYSTEM AND FISHERIES—J. HARE

documenting changes in distribution. The population center of many species in the southern part of the ecosystem has moved northeastward (Kleisner et al. 2016). In the northern part of the ecosystem, the population center of many species has moved southwestward. These sub-ecosystem differences are related to the complexity of the geology and oceanography in the ecosystem. The southern part of the ecosystem is a typical broad continental shelf; warming waters result in the thermal habitat moving poleward and into deeper water. The northern part of the ecosystem, the Gulf of Maine, is bathymetrically complex with deep basins, banks, and channels. The coolest water is observed in the deeper southwestern basins, and cold-water species appear to be moving into this area. These sub-ecosystem differences in distribution changes indicate the importance of physical characteristics of an ecosystem in influencing the response of species to changing ocean and climate conditions. Similar changes in distribution were observed in the late 1940s during the last warm period (Fig. SB3.1; Taylor et al. 1957; Friedland and Hare 2007).

Fisheries are also changing in the ecosystem. Fishery landings of some species are moving northward as the species themselves move northward (Pinsky and Fogarty 2012). As an example, lobster landings have shifted from Connecticut, New York, and New Jersey to Maine, partly as a result of warming temperatures and decreasing productivity in the south and increasing productivity in the north. This change in landings has greatly diminished the lobster fishery in southern New

England and resulted in a boom in Maine (Steneck and Wahle 2013). New fisheries are also developing in the region, including blueline tilefish and chub mackerel, species that historically occurred south of Cape Hatteras. A number of species are being captured by both commercial and recreational fisheries in new, predominantly more northern areas. There is also concern about the impact of ocean acidification on the region's fisheries. Laboratory and modeling studies have shown the potential for negative impacts on populations and fisheries (Talmage and Gobler 2010; Fay et al. 2017) but effects have yet to be attributed to observed changes in the region's living marine resources.

Changes in population productivity, population distribution, and fishing patterns are challenging some long-held spatial management strategies, including fixed spatial allocation of allowable catch and regional management, with species moving into new regions. These changes are also challenging the collection of fisheries data in the region. In the coming years, developing strategies to provide scientific advice for assessing and managing living marine resources in the face of changing ocean and climate conditions is going to present a major challenge to the stewardship of the nation's ocean resources and their habitat (Morrison and Termini 2016). To meet these challenges, NOAA Fisheries released a Fisheries Climate Science Strategy (Link et al. 2015), and a Regional Action Plan has been developed for the northeast U.S. shelf ecosystem (Hare et al. 2016).

2011). In some high latitude regions, sea ice formation, advection, and melt (e.g., Petty et al. 2014) can also influence SSS. Hence, relatively salty surface waters are observed in the subtropics where evaporation dominates, and fresher waters under the intertropical convergence zones (ITCZs) and in subpolar regions where precipitation dominates. Below the surface, fresher subpolar waters slide along isopycnals to intermediate depths and spread underneath saltier subtropical waters, which are in turn capped at low latitudes by fresher tropical waters (e.g., Skliris et al. 2014). Salinity changes in these layers can quantify the increase of the hydrological cycle associated with global warming over recent decades (Skliris et al. 2014). Below these layers lies salty North Atlantic Deep Water, formed mostly by open ocean convection, with salinity varying over decades (e.g., Yashayaev and Loder 2016). Fresher and colder Antarctic Bottom Waters, formed mostly in proximity to ice shelves, fill the abyss of

much of the ocean (Johnson 2008) and have been freshening in recent decades (e.g., Purkey and Johnson 2013). Salinity changes also have an effect on sea level (e.g., Durack et al. 2014) and the thermohaline circulation (e.g., Liu et al. 2017).

To investigate interannual changes of subsurface salinity, all available salinity profile data are quality controlled following Boyer et al. (2013) and then used to derive 1° monthly mean gridded salinity anomalies relative to a long-term monthly mean for years 1955–2012 (World Ocean Atlas 2013 version 2; WOA13v2; Zweng et al. 2013) at standard depths from the surface to 2000 m (Boyer et al. 2012). In recent years, the largest source of salinity profiles is the profiling floats of the Argo program (Riser et al. 2016). These data are a mix of real-time (preliminary) and delayed-mode (scientific quality controlled) observations. Hence, the estimates presented here could change after all data have been subjected to scientific

quality control. The SSS analysis relies on Argo data downloaded in January 2017, with annual maps generated following Johnson and Lyman (2012) as well as monthly maps of bulk (as opposed to skin) SSS data from BASS (Xie et al. 2014). BASS blends in situ SSS data with data from the *Aquarius* (Le Vine et al. 2014; mission ended in June 2015) and SMOS (Soil Moisture and Ocean Salinity; Font et al. 2013) satellite missions. BASS maps can be biased fresh around land (including islands) and should be compared carefully with in situ data-based maps at high latitudes before trusting features there. Despite the lower accuracies of satellite data relative to Argo data, their higher spatial and temporal sampling allows higher spatial and temporal resolution maps than are possible using in situ data alone. Salinity is measured as a dimensionless quantity and reported on the 1978 Practical Salinity Scale, or PSS-78 (Fofonoff and Lewis 1979).

2) SEA SURFACE SALINITY—G. C. Johnson and J. M. Lyman

The 2016 SSS anomalies (Fig. 3.7a, colors) reveal some large-scale patterns that largely held from 2004 to 2015 (e.g., Johnson et al. 2016, and previous *State of the Climate* reports). Regions around the subtropical salinity maxima are generally salty with respect to WOA13v2. While less clear in 2016 than in previous years, some high-latitude, low-salinity regions are slightly fresher overall than WOA13v2, primarily in portions of the subpolar gyres of the North Pacific and North Atlantic. These multiyear patterns are consistent with an increase in the hydrological cycle (e.g., more evaporation in drier locations and more precipitation in rainy areas) over the ocean, as expected in a warming climate (Rhein et al. 2013). The large, relatively fresh patch in 2016 in the eastern Indian Ocean north of 30°S has been present back to 2011 (Johnson and Lyman 2012). It originally resulted from high precipitation owing to the interaction of the strong 2010–12 La Niña with other climate patterns (Fasullo et al. 2013).

Sea surface salinity changes from 2015 to 2016 (Fig. 3.7b, colors) strongly reflect 2016 anomalies in evaporation minus precipitation (see Fig. 3.12). Advection by anomalous ocean currents (see Fig. 3.18) also plays a role in SSS changes. Prominent large-scale SSS changes from 2015 to 2016 reflect salinification on either side of Central America, east of the Philippines, and in the Labrador Sea (Fig. 3.7b). Freshening during this time period is prominent around the Maritime Continent, in the Bay of Bengal, in the northeast tropical Pacific fresh pool, in portions of the subtropical and subpolar North Pacific, and east of Greenland. The tropical Pacific changes are likely owing to the

transition from the strong 2015/16 El Niño to weak La Niña conditions later in 2016.

Seasonal variations of SSS anomalies in 2016 (Fig. 3.8) from BASS (Xie et al. 2014) show that fresh anomalies in the eastern Indian Ocean peak in March–May. Fresh anomalies increased in the center of the subpolar North Pacific over the course of the year, with salty anomalies in the eastern North Pacific peaking in June–August. In the equatorial Pacific

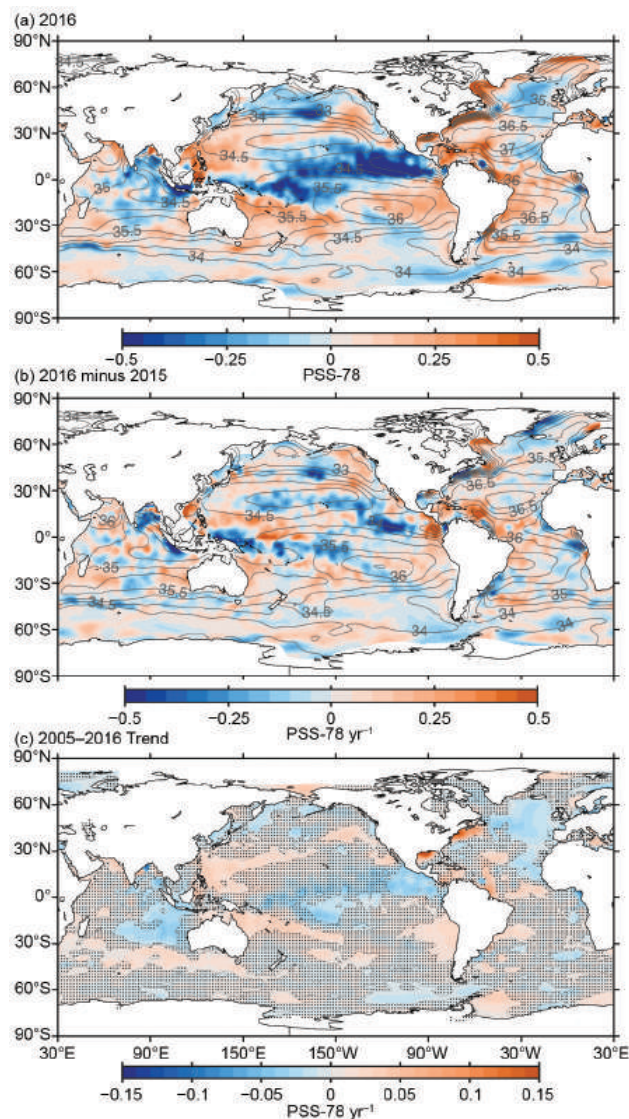


FIG. 3.7. (a) Map of the 2016 annual surface salinity anomaly (colors, PSS-78) with respect to monthly climatological 1955–2012 salinity fields from WOA13v2 [yearly average (gray contours at 0.5 intervals), PSS-78]. (b) Difference of 2016 and 2015 surface salinity maps (colors, PSS-78 yr⁻¹). White ocean areas are too data-poor (retaining <80% of a large-scale signal) to map. (c) Map of local linear trends estimated from annual surface salinity anomalies for 2005–16 (colors, PSS-78 yr⁻¹). Areas with statistically insignificant trends are stippled. All maps are made using Argo data.